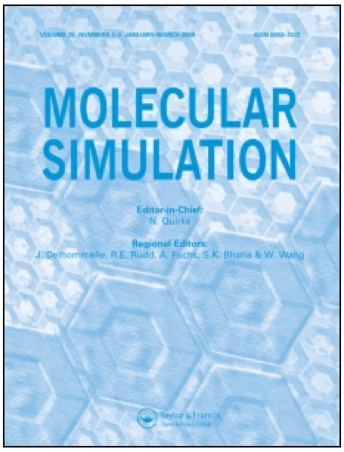

Molecular Simulation
Publication details, including instructions for authors and subscription information:
http://www.informaworld.com/smpp/title~content=t713644482

The Miscibility of Copper Halides Using a Three-Body Potential. I. CuCl$_{\text{<i>x</i>}}$Br$_{\text{1-<i>x</i>}}$ Crystal

W. Sekkal[a]; A. Laref[a]; A. Zaoui[b]; H. Aourag[a]; M. Certier[b]
[a] Computational Materials Science Laboratory, Physics Department, University of Sidi Bel-Abbes, Algeria [b] L. P. L. I. 08 Rue Marconi, Cedex 3, France

To cite this Article Sekkal, W. , Laref, A. , Zaoui, A. , Aourag, H. and Certier, M.(1999) 'The Miscibility of Copper Halides Using a Three-Body Potential. I. CuCl$_{\text{<i>x</i>}}$Br$_{\text{1-<i>x</i>}}$ Crystal', Molecular Simulation, 23: 2, 127 — 142

To link to this Article: DOI: 10.1080/08927029908022117

URL: http://dx.doi.org/10.1080/08927029908022117

Molecular Simulation, 1999, Vol. 23, pp. 127–142
Reprints available directly from the publisher
Photocopying permitted by license only

Published by license under
the Gordon and Breach Science
Publishers imprint.
Printed in Malaysia.

THE MISCIBILITY OF COPPER HALIDES USING A THREE-BODY POTENTIAL.
I. $CuCl_xBr_{1-x}$ CRYSTAL

W. SEKKAL[a], A. LAREF[a], A. ZAOUI[b],
H. AOURAG[a],* and M. CERTIER[b]

[a]*Computational Materials Science Laboratory, Physics Department, University of Sidi Bel-Abbes, 22000-Algeria;* [b]*L. P. L. I. 08 Rue Marconi, Technopôle 2000, 57078-Metz Cedex 3 France*

(accepted May 1999)

Mixed $CuCl_xBr_{1-x}$ crystals are studied using a Tersoff potential. Structural and elastic properties of the solid solution are calculated and are in good agreement with experiments. Various thermodynamic quantities including thermal expansion coefficient, heat capacity, and Grüneisen coefficient are also predicted.

Keywords: Tersoff potential; solid solution; Grüneisen coefficient; copper halide

I. INTRODUCTION

Copper halides show promise as photosensitive and semiconductive materials and catalysts for organic reactions. Recently, they found renewed interest because of the possibility of producing microcrystals [1]. The copper halides CuCl and CuBr crystallize under ambient conditions in the zinc-blende structure. Most of the work in this field has been carried out on nominally pure materials. Recently, more attention was given to solid solution of copper halides. Bouhafs *et al.* [2] have studied electronic and optical properties of $CuCl_xBr_{1-x}$ and using a tight-binding method including

---

*Corresponding author.

d electron orbitals on the cation site. A close look at the structural properties of isovalent I-VII semiconductor alloys, such as CuCl-CuBr and CuBr-CuI, made possible by more recent measurements [3, 4], reveals, however, that these alloys form a completely solid solution. X-ray diffraction patters of these alloy systems indicated a cubic zinc-blende structure, and showed that the lattice parameter changed linearly with alloy concentration without changes in the crystal structure. Nuclear magnetic resonance (NMR) spectra [3] in a completely solid solution of CuCl-CuBr and CuBr-CuI appear to correspond to the overlapping peaks of five structural species with the lattice sites of C_{1v}, C_{2v}, C_{3v}, or T_d symmetries. These reflect distinct contributions by the five local atomic arrangements of the two cation atoms that are neighbour to Cu. Simple symmetry preserving nonstructural theories do not represent such distinct effects associated with the existence of a distribution of low symmetry environments. For instance, it is assume that the average of a distribution of a low symmetry configuration can be replaced by an effective high symmetry configuration. This can have significant implications for the description of optical and structural properties.

We present in this work the miscibility of $CuCl_xBr_{1-x}$ crystal for $x = 0.25$, 0.5 and 0.75 using a three-body potential (Tersoff model) which enabled successful calculations of several structural properties of solid CuCl and CuBr [5]. Our calculations are compared with the experimental measurements of Endo *et al.* [3] using NMR and X-ray diffraction. Various thermodynamic properties are also predicted such as the thermal expansion coefficient, heat capacity and Grüneisen coefficient.

II. DETAILS OF CALCULATIONS

Among the many empirical model potentials that have been developed for tetrahedral semiconductors, that of Tersoff has been the most successful in that it reproduces many of elemental semiconductors properties particularly for silicon [6] and carbon [7]. Another form is developed for multicomponent systems [8] to treat mixtures of these elements. The form of the energy E, between two neighboring atoms i and j, is taken to be [8]

$$E = \sum_i E_i = \frac{1}{2} \sum_{i \neq j} V_{ij}, \tag{1}$$

with

$$
\begin{aligned}
V_{ij} &= f_C(r_{ij})[a_{ij} f_R(r_{ij}) + b_{ij} f_A(r_{ij})], \\
f_R(r_{ij}) &= A_{ij} \exp(-\lambda_{ij} r_{ij}), \\
f_A(r_{ij}) &= -B_{ij} \exp(-\mu_{ij} r_{ij}), \\
f_C(r_{ij}) &= \begin{cases} 1 & r_{ij} < R_{ij} - D_{ij} \\ \dfrac{1}{2} - \dfrac{1}{2}\sin\left[\frac{\pi}{2}\frac{(r_{ij}-R_{ij})}{D_{ij}}\right] & R_{ij} - D_{ij} < r_{ij} < R_{ij} + D_{ij} \\ 0 & r_{ij} > R_{ij} + D_{ij} \end{cases}
\end{aligned}
\tag{2}
$$

b_{ij} is the many-body order parameter describing how the bond-formation energy is affected by local atomic arrangement due to the presence of other neighboring atoms (the k atoms). It is a many-body function of the positions of atoms i, j, and k. It has the form

$$
b_{ij} = \chi_{ij}\left(1 + \beta_i^n \zeta_{ij}^{n_i}\right)^{\frac{-1}{2n_i}} \tag{3}
$$

with

$$
\begin{aligned}
\zeta_{ij} &= \sum_{k(\neq i,j)} f_C(r_{ik}) g(\theta_{ijk}) \exp\left[\lambda_3^3 (r_{ij} - r_{ik})^3\right] \\
g(\theta_{ijk}) &= 1 + \frac{c_i^2}{d_i^2} - \frac{c_i^2}{d_i^2 + (h_i - \cos\theta_{ijk})^2} \\
a_{ij} &= \left(1 + \alpha^n \eta_{ij}^n\right)^{\frac{-1}{2n_i}} \\
\eta_{ij} &= \sum_{k(\neq i,j)} f_C(r_{ik}) \exp\left[\lambda_3^3 (r_{ij} - r_{ik})^3\right]
\end{aligned}
$$

$$
\lambda_{ij} = \frac{(\lambda_i + \lambda_j)}{2} \tag{4}
$$

$$
\mu_{ij} = \frac{(\mu_i + \mu_j)}{2} \tag{5}
$$

$$
A_{ij} = (A_i A_j)^{1/2} \tag{6}
$$

$$
B_{ij} = (B_i B_j)^{1/2} \tag{7}
$$

ζ is called the effective coordination number and $g(\theta_{ijk})$ is a function of the angle between r_{ij} and r_{ik} that has been fitted to stabilize the tetrahedral structure. We note that λ_3 and α are put equal to zero [9].

χ is a parameter which strengthens or weakens the heteropolar bonds, relative to the value obtained by simple interpolation.

Tersoff parameters for CuCl and CuBr were proposed recently [5]. From these values and using the above Eqs. (1 – 7), we have calculated the potential parameters (A, B, λ, μ, n, h, β, c, d) for $CuCl_{0.5}Br_{0.5}$. On the basis of the transferability of the Tersoff potential [5, 10], all the parameters for $CuCl_{0.25}Br_{0.75}$ and $CuCl_{0.75}Br_{0.25}$ have been kept constant except the cut-off R and χ which are adjusted to ensure the stability of each structure. All parameters are listed in Table I.

Using Monte Carlo calculations (MC), the interactions are described for different concentrations by the Tersoff potential. In our simulation, we assume that the system is treated as two-components (CuCl and CuBr). Indeed, CuCl and CuBr are considered as an equivalent one-component system.

Initially, CuCl and CuBr are always located at the nodes of a zinc-blende structure interacting *via* the Tersoff potential. The MC simulation is performed in the following manner (for more details, see reference [11]). A particle at position r_i is chosen and then we attempt to produce a new status at a slightly altered position r'_i. The acceptance or rejection of this attempt is done is *via* the usual Metropolis method.

Assuming that CuCl and CuBr have the same size and shape and with neclecting the freedom of orientation of molecules, we calculate the entropy of mixing using the classical formula for a totally disordered solution:

$$S = R(x_C \ln(x_C) + x_{BN} \ln(x_{BN})) \tag{8}$$

Where x is the molar concentration.

TABLE I The adjusted Tersoff parameters for $CuCl_{0.25}Br_{0.75}$, $CuCl_{0.5}Br_{0.5}$ and $CuCl_{0.75}Br_{0.25}$

	$CuCl_{0.25}Br_{0.75}$	$CuCl_{0.5}Br_{0.5}$	$CuCl_{0.75}Br_{0.25}$
A(eV)	142.473	142.473	142.473
B(eV)	29.1320	29.1320	29.1320
λ(Å^{1})	1.8822	1.8822	1.8822
μ(Å^{1})	0.9361	0.9361	0.9361
n	0.78367	0.78367	0.78367
h	−0.33331	−0.33331	−0.33331
β	10999×10^{-6}	10999×10^{-6}	10999×10^{-6}
c	1.0039×10^{-5}	1.0039×10^{-5}	1.0039×10^{-5}
d	16.0285	16.0285	16.0285
R(Å)	2.930	2.957	2.890
D(Å)	0.15	0.15	0.15
χ	0.9970	0.9855	1.0355

The internal energy of the system is a sum of interactions between pairs of CuCl-CuCl, CuBr-CuBr and CuCl-CuBr. For the random case, the difference in internal energy between the alloy and the mixture of pristine components can be written as:

$$\begin{aligned}\Delta u = {} & x_{\mathrm{CuCl}}x_{\mathrm{CuCl}}u_{\mathrm{CuCl-CuCl}}\frac{Nz}{2} \\ & + x_{\mathrm{CuBr}}x_{\mathrm{CuBr}}u_{\mathrm{CuBr-CuBr}}\frac{Nz}{2} \\ & + x_{\mathrm{CuCl}}x_{\mathrm{CuBr}}u_{\mathrm{CuCl-CuBr}}Nz \\ & - x_{\mathrm{CuCl}}u_{\mathrm{CuCl-CuCl}}\frac{Nz}{2} \\ & - x_{\mathrm{CuBr}}u_{\mathrm{CuBr-CuBr}}\frac{Nz}{2} \end{aligned} \tag{9}$$

where z denotes the number of nearest neighbors, N the number of molecules in the system and u the intermolecular potential.

Using Eqs. (8) and (9), the free energy of mixing is directly calculated. It is the difference between the energy and entropy terms:

$$F = \Delta u - TS \tag{10}$$

If $\mathrm{CuCl}_x\mathrm{Br}_{1-x}$ solid solutions were stable at all concentrations, the free energy of mixing F for the system would be negative.

III. RESULTS AND DISCUSSIONS

In Figure 1, we present the result of our calculations based on a MC method. It appears that the entropic contribution to the free energy is responsible for the mixing effect. Indeed, the magnitude of the entropy term is larger, resulting in negative values for the Helmholtz energy of mixing. Consequently, $\mathrm{CuCl}_x\mathrm{Br}_{1-x}$ solid solution can be considered stable at all concentrations.

X-ray diffraction [3] patters of the $\mathrm{CuCl}_x\mathrm{Br}_{1-x}$ alloy indicated a cubic zinc-blende structure, and showed that the lattice parameters changed linearly with Cl : Br concentration ratios without changes in the crystal structure. In order to obtain more informations about the structural and thermodynamic properties of $\mathrm{CuCl}_{0.25}\mathrm{Br}_{0.75}$, $\mathrm{CuCl}_{0.5}\mathrm{Br}_{0.5}$ and $\mathrm{CuCl}_{0.75}\mathrm{Br}_{0.25}$, we run a molecular-dynamics simulation using Tersoff potential with 216 molecules. This system is allowed to relax into equilibrium by integrating the equations of motion through a fifth-order Gear-Predictor-Corrector

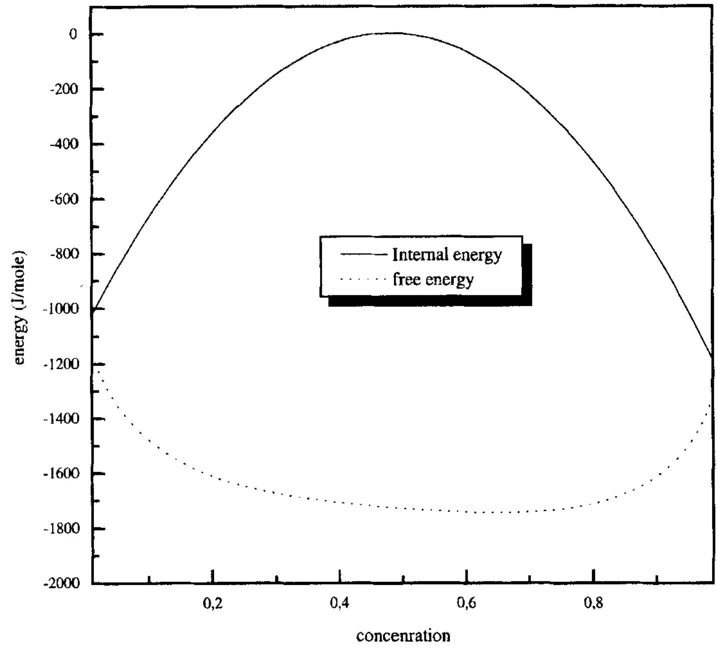

FIGURE 1 Free energy of mixing *versus* molar concentrations of $CuCl_xBr_{1-x}$.

algorithm with a time step $h = 4.09$ fs. The simulation is carried out within the canonical *NVT*-ensemble where the temperature control is investigated using Andersen's method [12]. After 82 ps, different properties are computed along the trajectory of the system in phase space.

Figure 2(a, b, c) display the pair distribution function $g(r)$ for $CuCl_{0.25}Br_{0.75}$, $CuCl_{0.5}Br_{0.5}$ and $CuCl_{0.75}Br_{0.25}$ alloy. The results for the fourth peaks listed in Table II are in good agreement with the experimental values of Endo *et al.* [3].

Figures 3(a, b, c) display the pressure *versus* the lattice parameter for $CuCl_{0.25}Br_{0.75}$, $CuCl_{0.5}Br_{0.5}$ and $CuCl_{0.75}Br_{0.25}$ in the zinc-blende structure. The curves are fitted to the Birch's equation of state [13] from which the equilibrium lattice parameter, the bulk modulus, and its derivative are obtained. From the results listed in Table III, we notice the agreement of the lattice parameter and the bulk modulus for the zinc-blende structure with the experimental data [3]. The accuracy is around 0.2% for the lattice parameter and about 1% for the bulk modulus. We see that the bulk modulus calculated from the equation of state is close to the predicted value based on its stoichiometry (see Fig. 4). This value is greater by 7.5% than for CuBr.

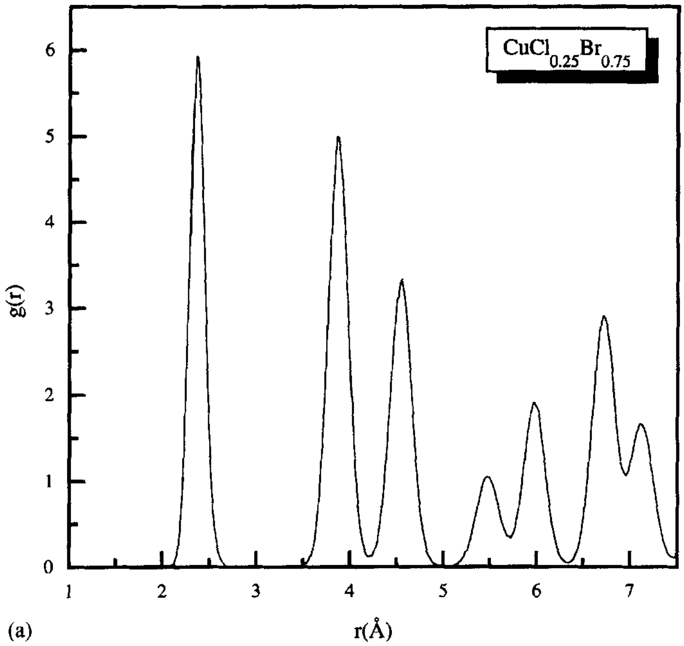

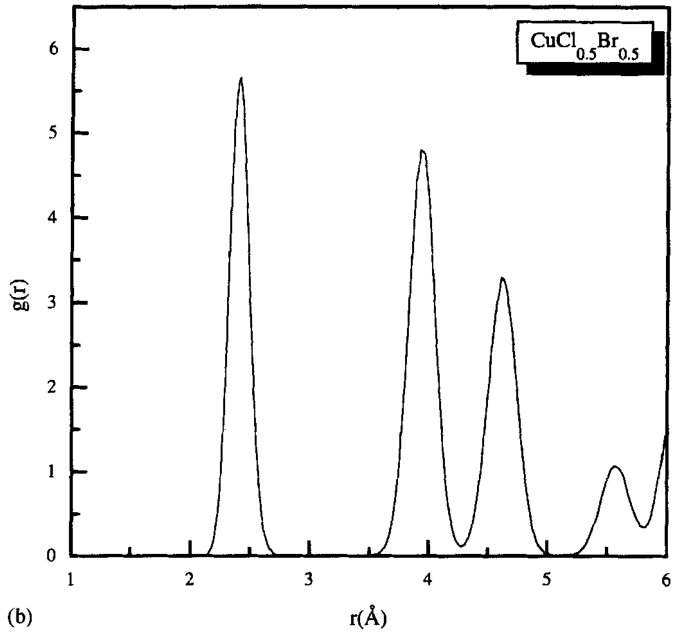

FIGURE 2 Pair correlation function for $CuCl_{0.25}Br_{0.75}$ (a) $CuCl_{0.5}Br_{0.5}$ (b) and $CuCl_{0.75}Br_{0.25}$ (c) at 300K.

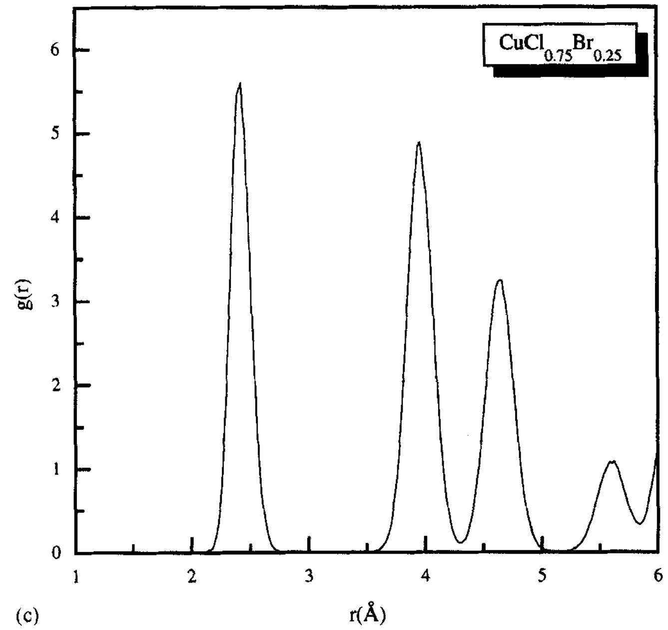

FIGURE 2 (Continued).

TABLE II Peak distances and number of pairs for $CuCl_{0.25}Br_{0.75}$, $CuCl_{0.5}Br_{0.5}$ and $CuCl_{0.75}Br_{0.25}$

	$CuCl_{0.25}Br_{0.75}$		*$CuCl_{0.5}Br_{0.5}$*		*$CuCl_{0.75}Br_{0.25}$*		
Peak	*Distance (Å)*		*Distance (Å)*		*Distance (Å)*		*Number of pair*
1st	2.373[a]	2.381[b]	2.413[a]	2.405[b]	2.425[a]	2.431[b]	3.97[a]
2nd	3.873[a]	3.888[b]	3.955[a]	3.927[b]	3.958[a]	3.970[b]	12.00[a]
3rd	4.549[a]	4.559[b]	4.609[a]	4.606[b]	4.649[a]	4.655[b]	12.00[a]
4th	5.488[a]	5.499[b]	5.564[a]	5.555[b]	5.626[a]	5.615[b]	6.02[a]

[a] Present work.

[b] Calculated from experimental result taken from Reference [3].

This is shown in Figure 5 where we give pressure *versus* volume for CuCl, CuBr and $CuCl_{0.5}Br_{0.5}$.

In Figure 6, we plot the lattice parameter for $CuCl_xBr_{1-x}$ solid solution. We notice that for all concentrations ($x = 0.25, x = 0.5$ and $x = 0.75$), the calculated lattice parameters are in good agreement with experimental results for which the variation is linear and follow the Vegard's Law very closely. As conclusion, we can say that there is an ideal mixing between CuCl and CuBr.

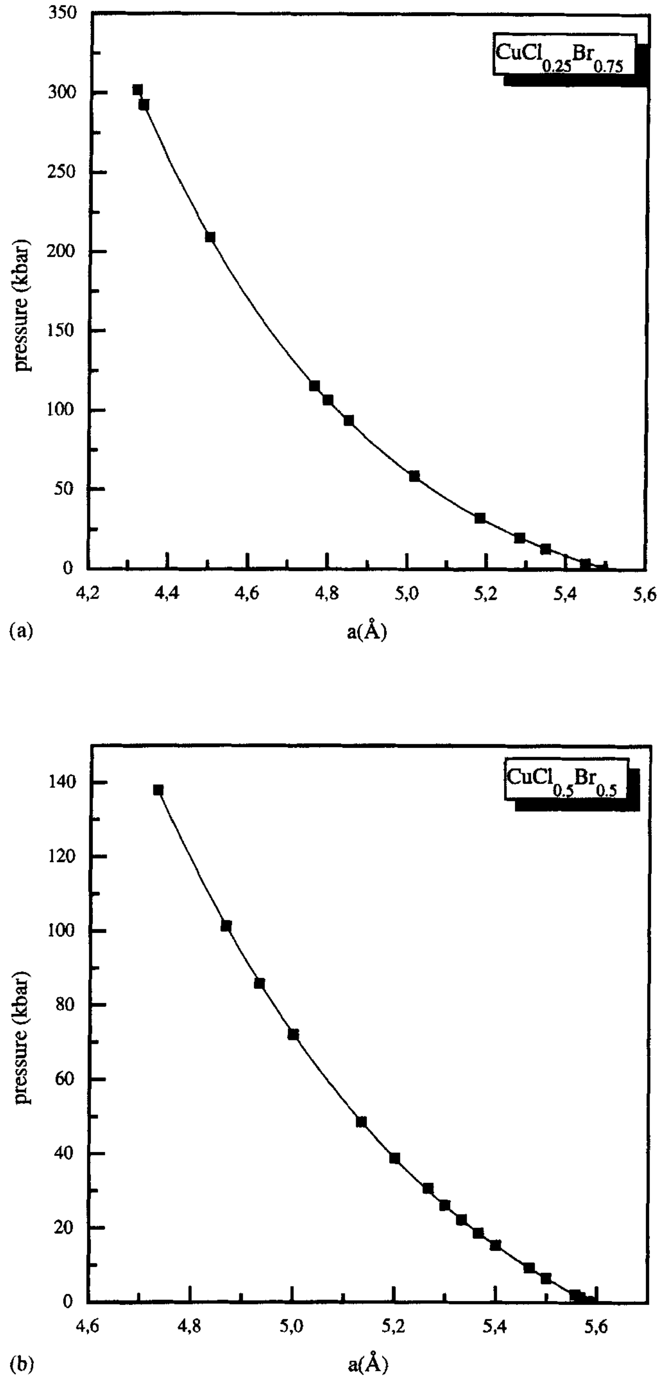

FIGURE 3 The pressure of the system as a function of lattice parameter for $CuCl_{0.25}Br_{0.75}$ (a), $CuCl_{0.5}Br_{0.5}$ (b) and $CuCl_{0.75}Br_{0.25}$ (c).

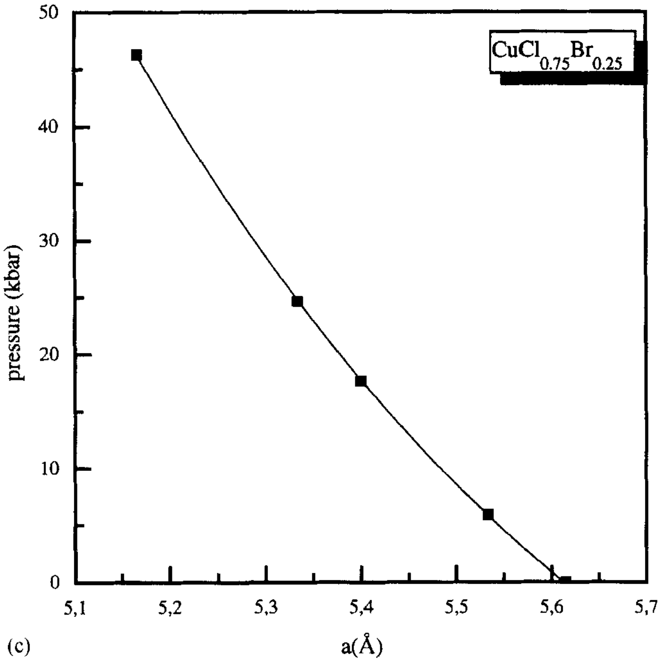

(c)

FIGURE 3 (Continued).

TABLE III Structural properties of $CuCl_{0.25}Br_{0.75}$, $CuCl_{0.5}Br_{0.5}$ and $CuCl_{0.75}Br_{0.25}$

	CuCl	$CuCl_{0.25}Br_{0.75}$		$CuCl_{0.5}Br_{0.5}$		$CuCl_{0.75}Br_{0.25}$		*CuBr*
a(Å)	5.47[a]	5.514[c]	5.499[d]	5.560[c]	5.555[d]	5.612[c]	5.615[d]	5.68[a]
B(Mbar)	0.403[a]	0.367[c]	0.365[e]	0.374[c]	0.370[e]	0.385[c]	0.389[e]	0.348[a]
B'	11.25[a]	11.97[c]		6.11[c]		9.38[c]		10.35[a]
$C_v(k_B)$		3.1[c]		3.1[c]		3.2[c]		
γ		1.08[c]		1.07[c]		0.91[c]		
$\alpha_l\ (10^{-5}\ K^{-1})$	1.38[b]	2.02[c]		1.90[c]		1.58[c]		1.61[b]

[a] [5],
[b] [14],
[c] Present work,
[d] [3],
[e] from Vegard's Law.

We are interesting now in calculating the thermodynamics properties of $CuCl_xBr_{1-x}$ for $x = 0.25$, $x = 0.5$, and $x = 0.75$.

In MD simulation, the linear thermal expansion coefficient α_l can be computed directly from the definition

$$\alpha_l = \frac{1}{a}\frac{\partial a}{\partial T}\bigg|_P \qquad (11)$$

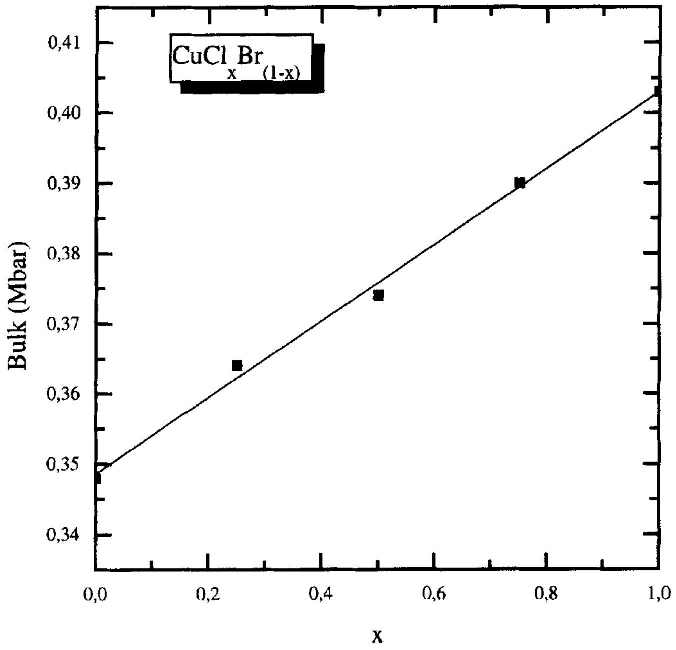

FIGURE 4 The bulk modulus *versus* concentration of $CuCl_xBr_{1-x}$. The solid line is prediction of ideal mixing according to the Vegard's Law. Squares correspond to our results.

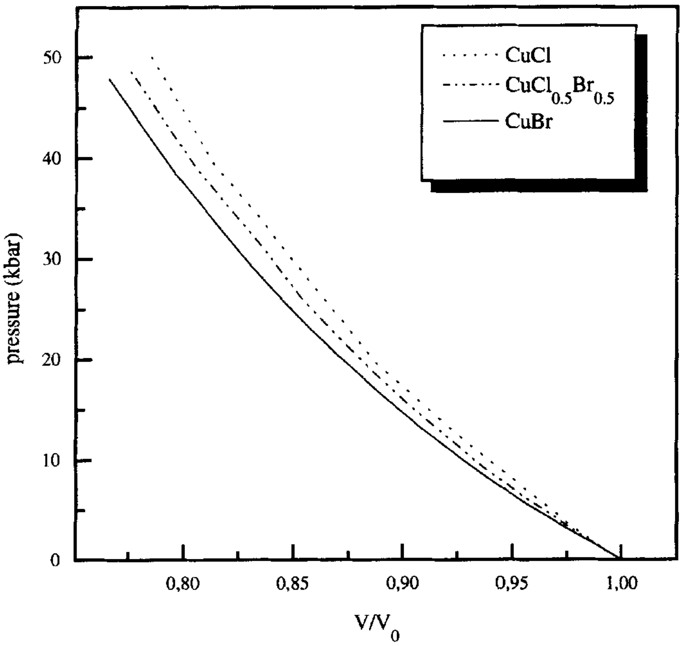

FIGURE 5 The pressure *versus* volume for CuCl, CuBr and $CuCl_{0.5}Br_{0.5}$.

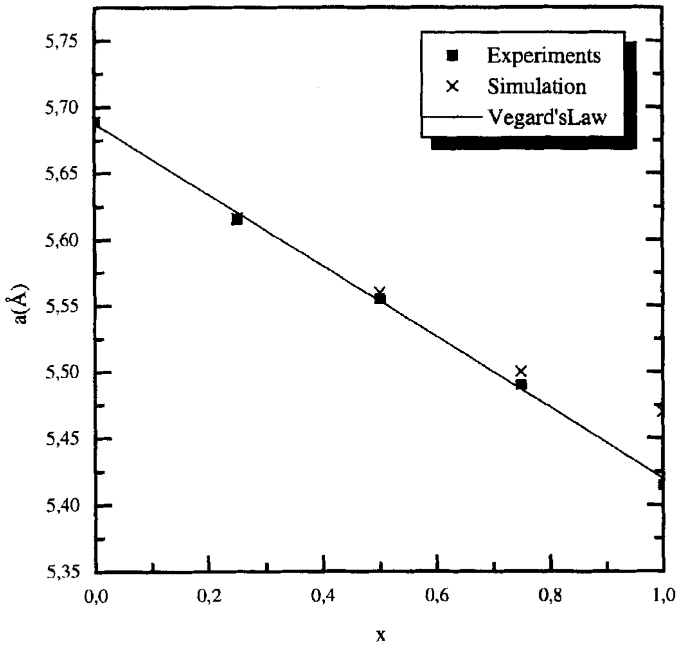

FIGURE 6 The lattice parameter *versus* concentration of $CuCl_xBr_{1-x}$. The solid line is a prediction of ideal mixing according to the Vegard's Law. Squares correspond to our simulation data which are compared with experiments (Crosses).

where a is the lattice parameter. Therefore, we consider the temperature variation of the lattice constant at zero pressure (see Figs. 7a, b, c). A molecular-dynamics simulation is performed in an NVT ensemble at each temperature to equilibrate the system and then to determine the corresponding zero pressure lattice constant.

From the slope of the total energy *versus* temperature curve (see Figs. 8 a, b, c), we can estimate the specific heat of the system according to the following equation:

$$C_v = \left| \frac{\partial E}{\partial T_v} \right| \tag{12}$$

Grüneisen constant can also be calculated using the following equation:

$$\gamma = \frac{3BV\alpha_l}{C_v} \tag{13}$$

where V is the molar volume.

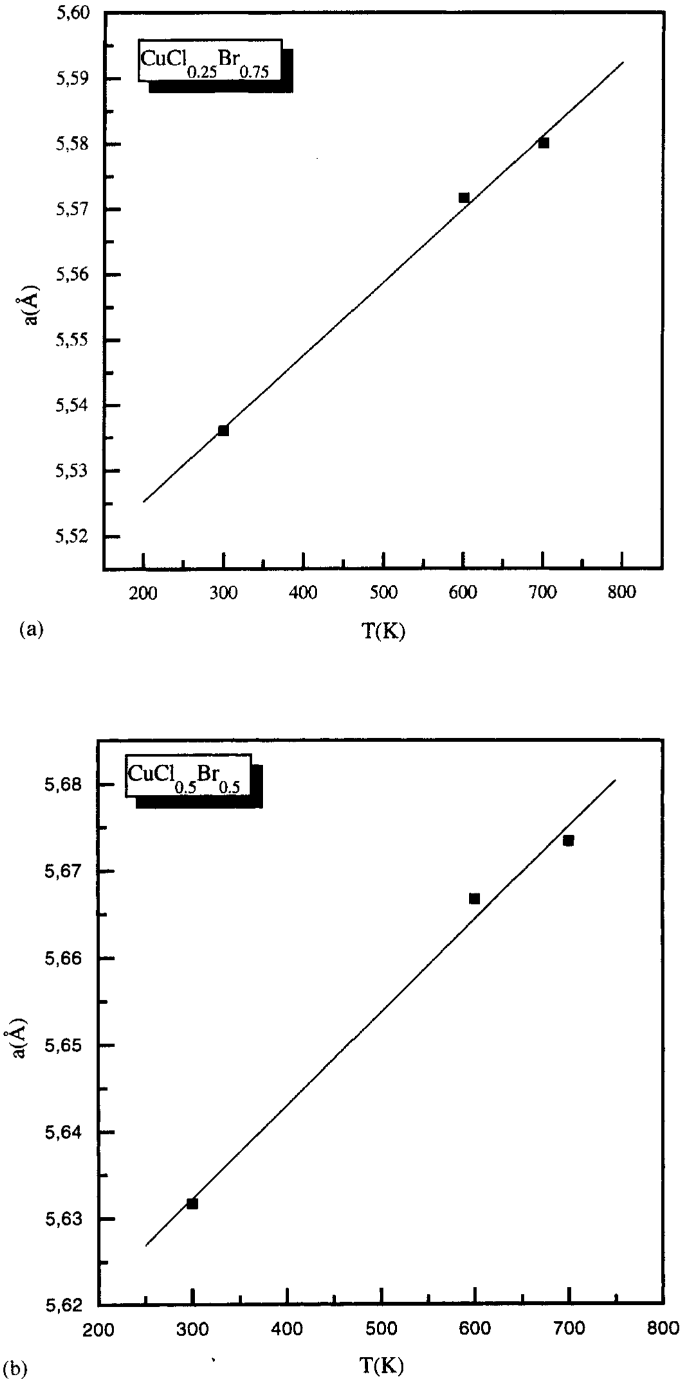

FIGURE 7 The lattice parameter as a function of temperature for $CuCl_{0.25}Br_{0.75}$ (a), $CuCl_{0.5}Br_{0.5}$ (b) and $CuCl_{0.75}Br_{0.25}$ (c).

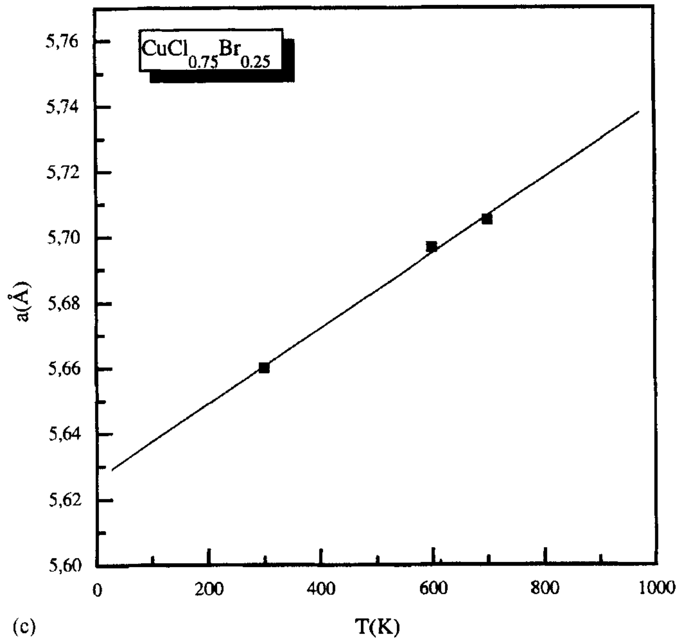

FIGURE 7 (Continued).

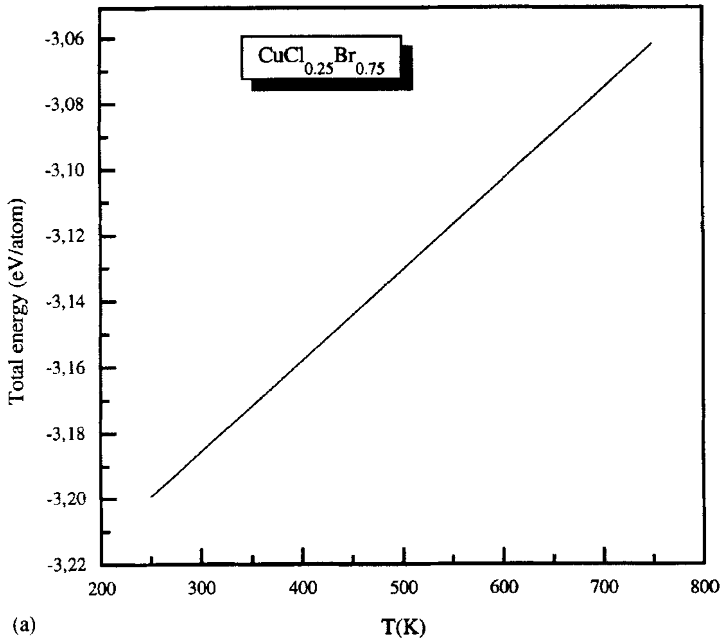

FIGURE 8 The total energy as a function of temperature for $CuCl_{0.25}Br_{0.75}$ (a), $CuCl_{0.5}Br_{0.5}$ (b) and $CuCl_{0.75}Br_{0.25}$ (c).

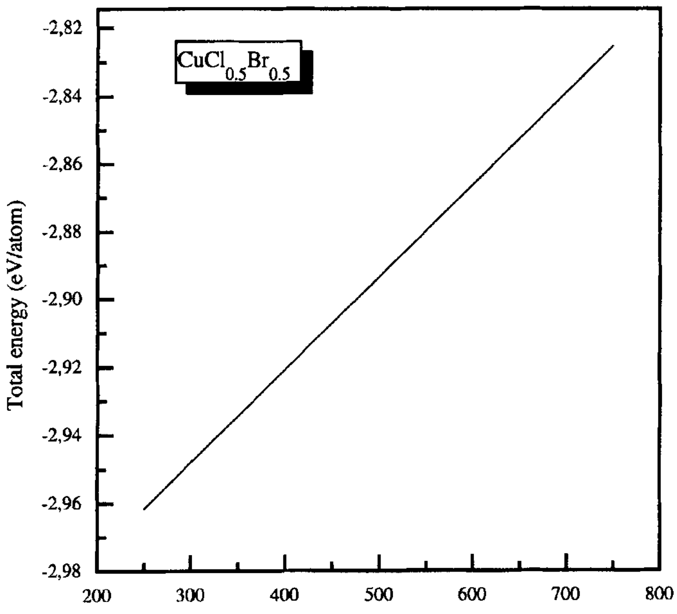

(b)

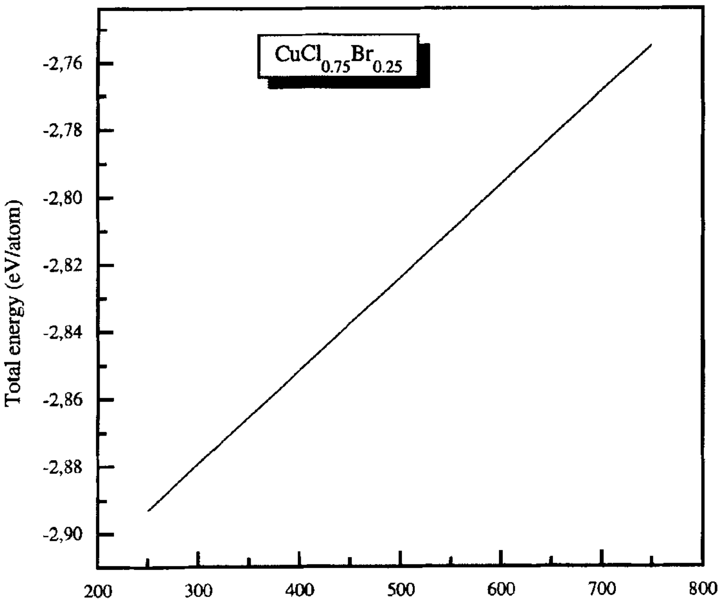

(c)

FIGURE 8 (Continued).

All the predicted thermodynamic properties are listed in Table III. The specific heat for $CuCl_{0.25}Br_{0.75}$, $CuCl_{0.5}Br_{0.5}$ and $CuCl_{0.75}Br_{0.25}$ alloy is around 3.1 k_B. This constant value corresponds to the classical Dulong-Petit result (3 k_B), which is obtained at high temperatures for all solids.

IV. CONCLUSION

We have presented a simulation method for the calculation of the structural and elastic properties of $CuCl_xBr_{1-x}$ alloy. The calculated lattice parameters, the bulk modulus, and its derivative are in good agreement with available experimental measurements. Different thermodynamics properties such as heat capacity, mode Grüneisen parameter, and linear thermal expansion coefficient are predicted.

References

[1] Masumoto, Y., Kawamura, T. and Era, K. (1993). "Biexciton lasing in CuCl quantum dots", *Appl. Phys. Lett.*, **62**, 225.

[2] Bouhafs, B., Heireche, H., Sekkal, W., Aourag, H. and Certier, M. (1998). "Electronic and optical properties of copper halides mixed crystal $CuCl_xBr_{1-x}$", *Phys. Lett. A*, **240**, 257.

[3] Endo, K., Yamamoto, K. and Deguchi, K. (1993). "Structure analysis of metal (I) halide mixed crystals by Cu MASNMR and X-ray diffraction methods. III. CuCl crystal", *J. Phys. Chem. Solids*, **54**, 357.

[4] Endo, K., Yamamoto, K. and Deguchi, K. (1993). "Structure analysis of metal (I) halide mixed crystals by MASNMR and X-ray diffraction methods-II. CuBr crystal", *J. Phys. Chem. Solids*, **54**, 15.

[5] Sekkal, W., Aourag, H. and Certier, M. (1998). "Molecular dynamics simulation of high pressure phases of CuCl and CuBr", *J. Phys. Chem. Solids*, **59**, 1293.

[6] Tersoff, J. (1988). "Empirical interatomic potential for silicon with improved elastic properties", *Phys. Rev. B*, **38**, 9902.

[7] Tersoff, J. (1988). "Empirical interatomic potential for carbon, with applications to amorphous carbon", *Phys. Rev. Lett*, **61**, 2879.

[8] Tersoff, J. (1989). "Modeling solid-state chemistry: interatomic potentials for multicomponent system", *Phys. Rev. B*, **39**, 5566.

[9] Tersoff, J. (1988). "New empirical approach for the structure and energy of covalent systems", *Phys. Rev. B*, **37**, 6991.

[10] Sekkal, W., Bouhafs, B., Aourag, H. and Certier, M. (1998). "Molecular-dynamics simulation of structural and thermodynamic properties of BN", *J. Phys. Condens. Matter*, **10**, 4975.

[11] Dünweg, B. and Landau, D. P. (1993). "Phase diagram and critical behavior of the Si-Ge unmixing transition: A Monte Carlo study of a model with elastic degrees of freedom", *Phys. Rev. B*, **48**, 14182.

[12] Anderden, H. C. (1980). "Molecular dynamics simulations at constant pressure and/or temperature", *J. Chem. Phys.*, **72**, 2384.

[13] Birch, F. J. (1978). "Finite strain isotherm and velocities for single-crystal and polycrystalline NaCl at high pressures 300 K", *J. Geophys. Res.*, **83**, 1257.

[14] Landolt-Börnstein, O., "Numerical data and functional relationships in science and technology", **22**, Springer-Verlag, Berlin 1986.